Development and Design of a Floating Type Ocean Current Turbine System

Yasushi Dodo[1](✉), Shigeki Nagaya[1], Tetsuo Okada[2], Makoto Toyoda[1], and Akio Ito[1]

[1] IHI Corporation, Kanagawa, Japan
yasushi_dodo@ihi.co.jp
[2] Faculty of Engineering, Yokohama National University, Yokohama, Japan

Abstract. Ocean currents are expected as future renewable energy resources. Recently various ideas are studied all over the world to utilize the power of this ocean current for generation of electricity. Application of various types of turbines has been proposed for this purpose, but very little examples have been reported with regard to actual demonstration in the natural ocean current environment.

The Kuroshio Current which flows through near Japan coast is one of the strongest ocean currents in the world. To utilize this plentiful energy, we developed the floating type ocean current turbine system "KAIRYU" under the support of NEDO (New Energy and Industrial Technology Development Organization), and we completed the 100 kW order turbine demonstration test in the natural Kuroshio Current.

In this paper, we report design methodologies and the results of the test. Especially we focus on the structural design to enable stable floatation in the water, the control of weight distribution and the center of floatation for balance, and the pressure-resistant design of the shell structure to secure water-tightness in the deep sea.

Keywords: Marine renewable energy · Offshore structure · Power generation · Ocean current · Kuroshio · Floating type ocean current turbine · Experiment in sea · KAIRYU

1 Introduction

Japan's Exclusive Economic Zone (EEZ) is the sixth largest in the world. Proceeding development of utilizing ocean renewable energy in the EEZ is required actively in terms of the reduction in greenhouse gas emissions and energy security. Ocean current such as Kuroshio flows stably almost all year near Japan. Accordingly, by using this Japanese own natural enormous energy, it is strongly expected to establish new clean and stable source of electric power.

On the other hand, there have been many studies on turbine system to utilize the power of ocean current for generation of electricity [1–5]. Some types were installed on the seabed, but to make the most of the Kuroshio Current spreading widely near the water surface, majority of the proposed systems was floating type tethered to the sea

T. Okada et al. (Eds.): PRADS 2019, LNCE 65, pp. 732–755, 2021.
https://doi.org/10.1007/978-981-15-4680-8_49

floor. Among them, Chen [1] discussed a large platform fitted with dozens of turbines. Finkl et al. [2] reported an open-center turbine application in the Straits of Florida, while Shirasawa et al. [3] proposed an energy farm consisting of many single rotor floaters with torque compensation using a float and a counterweight. Lo et al. [4] and Lai et al. [5] studied a floating system fitted with a large foil floater at the upper part of the floating body to induce dynamic lifting force.

In this study, we propose a twin-turbine floating system moored from the bottom of the sea (Fig. 1), attaching importance to the stable performance on electricity generation as well as the efficient installation and maintenance. A floating type turbine tethered to the sea floor enables easy maintenance by uplift to the surface of the sea through deballasting as shown in Fig. 1. In addition, because the turbine is located well beneath the water surface in the operating condition, it does not affect ship navigation in the area, and also it is not influenced by the wave forces, which may be very severe on the surface of the sea in case of a typhoon. Furthermore, by floating around the relevant depth of the sea, the turbine can effectively utilize a wide and deep Kuroshio Current.

In this paper, we first present the basic design of the system and describe the pilot studies with regard to the design concept and the strength of the turbine blades and the pressure vessel under the deep sea pressure. Next, design and construction of the 100 kW demonstration machine are explained. Demonstration tests were carried out with regard to the performance of electricity generation, mooring, and strength of the floating body. In the final sections, we describe the test results, and especially elaborate on the results of strain measurements in comparison to the structural design and the finite element analysis, followed by the concluding remarks.

Fig. 1. Concept view of floating type ocean current turbine system

2 Basic Design

2.1 Design Concept

As explained in the Introduction, the ocean current turbine system operates beneath the sea surface moored from the bottom of the sea, and is uplifted to the water surface when maintenance is required. Being installed in deep water, it can tap into the enormous ocean current energy from the wide ocean area available for power generation.

The system adopts horizontal-axis turbine generators, and as such, it is necessary to cancel the rotor torque so that the floater attitude is effectively controlled during operation. So we adopted two-turbine system so that the torque in the left and the right cancels each other. The turbines and the floater were designed to the downwind type, rotating around the mooring anchor point according to the flow direction. Therefore, this system can be applied in any current direction without active control (see Fig. 2).

Thus, the ocean current turbine system can achieve stable floatation in the middle layer of the sea, without significant influence from the surface waves.

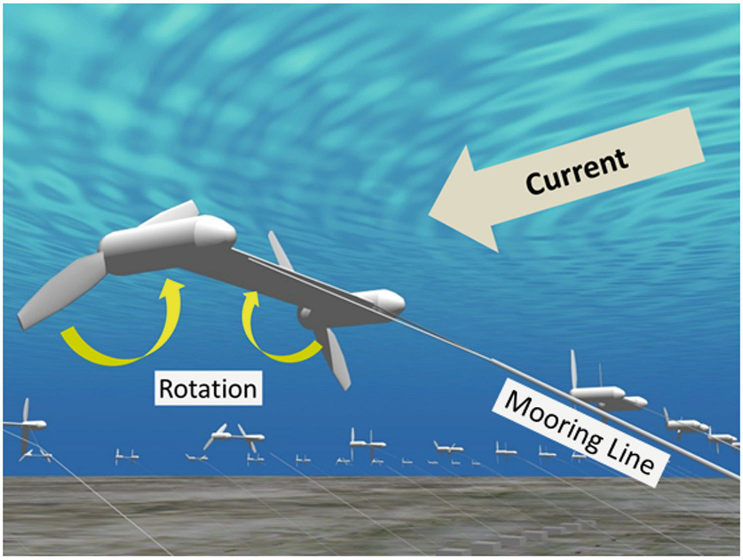

Fig. 2. Floating type ocean current turbine system

2.2 Pilot Study on Design Concept

A scale model pilot test was conducted to confirm the design concept as explained in the previous section. A model with a 1/25 scale about the blade diameter (Fig. 3) was fabricated and moored in the sea, and its behavior in the water was observed.

The dimensions of this scale model are about 1.8 m in length and 2 m in width, with turbine blades of 1.5 m in diameter. This scale model is equipped with a buoyancy adjustment device, an attitude adjustment device and a blade pitch control device to study the movement of the demonstration machine.

This pilot test was carried out both in a water tank and in the actual sea. Firstly, the water tank test was conducted at IHI's towing tank to confirm the stability in the stationary flow (The angle within $\pm 5^\circ$ deviation from the target and the depth within 25% deviation from the target). Then, the actual sea test was conducted at the sea area of Numazu in Shizuoka Prefecture to confirm the stable performance of the floating body in waiting at the surface of the sea, ballasting under the sea and starting of the turbine. As a result of this study, it was found that the basic concept works. In addition, it was found that the floating body becomes unstable when the center of gravity is close to the center of floatation, and thus the geometrical relationship of the center of gravity and the center of floatation is very important in the water.

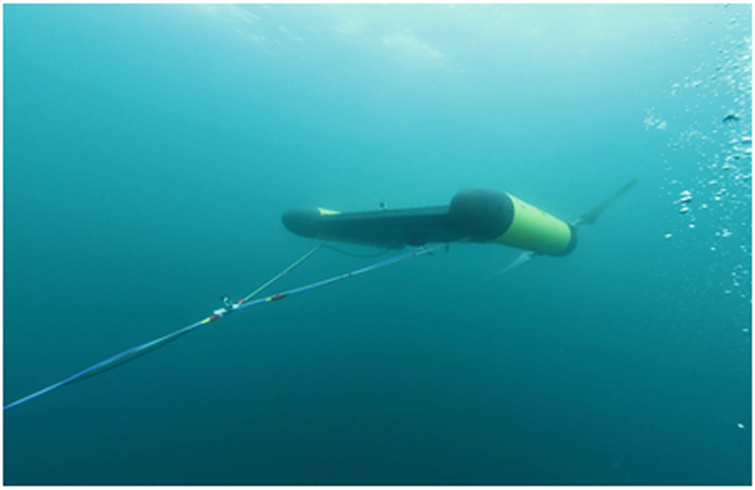

Fig. 3. 1/25 scale design concept model

2.3 Pilot Study on Turbine Blades

The material of the turbine blades was planned to be G-FRP. However, there was no established strength data of a very large blade similar to that used for windmills, working in the ocean current. So static strength test and destruction test of a 5 m scale turbine blade (Fig. 4) were carried out, and strength enough was confirmed. In the static strength test, the model of the turbine blade was simply supported by rigid walls, and loaded by two hydraulic cylinder at the two points between the supports to simulate the actual bending moment in the operation.

A turbine blade is designed for the purpose of getting energy from an ocean current. Its large deformation deteriorates the performance, and should be avoided even in the intact condition. From our preliminary study we assumed that the deformation should be within 5% of the span length. As a result of this test, the deformation was about 2% under the operational load, showing that no performance reduction is expected due to deformation. The cost of the blades was also confirmed to be within an expected level.

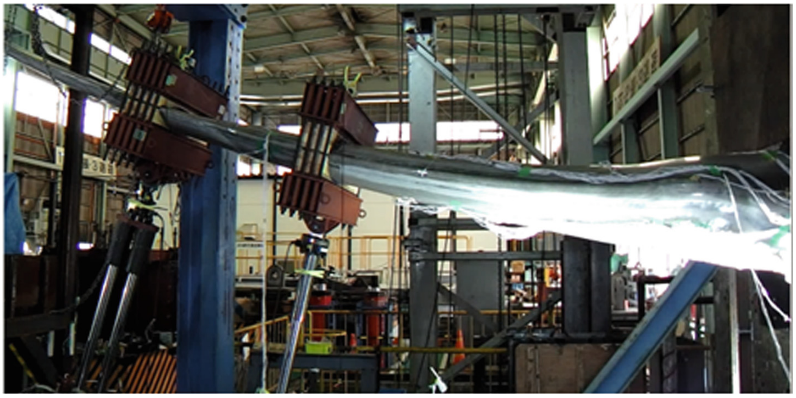

Fig. 4. Static strength test for 5 m scale turbine blade

2.4 Pilot Study on Performance of the Pressure Vessel in the Deep Sea

To achieve stable floatation in the water, the pressure-resistant design of the shell structure to secure water-tightness in the deep sea is very important. First, taking account of the heavy pressure in the deep sea down to 100 m depth, strength of the shell structure is of primary importance. In addition, there are several flange joints on the shell for human access and maintenance of the equipment. Actually a man hole is necessary to enable human access for maintenance, and in some cases large equipment should be taken out or carried in for maintenance. Thus, water-tightness of these flange joints is very important.

Therefore, to confirm strength and water-tightness of the pressure vessel, a mock-up model of the main structure was fabricated with the same diameter and the same structural and joint arrangement as the target demonstration machine, and the pressure test was carried out at the depth of 100 m (Fig. 5). It was confirmed that there are no problems with regard to strength and water-tightness of the shell structure. Strain gauges were arranged around the shell structure of this mock-up model, and the results were compared with the results of finite element analysis. Details of this comparison will be explained in Sect. 5.2.

Fig. 5. Pressure test with using mock-up model

3 Development of the Demonstration Machine

3.1 Design

From the feedback of the pilot studies as explained in the previous chapter, we established the basic design of the demonstration machine. To keep stabilized attitude of the floater in the water, the demonstration machine was fitted with two side turbine pods and a center pod as shown in Fig. 6. The center pod with a water ballast tank was arranged at a higher position than the two turbine pods, so that the floating center is located sufficiently higher than the center of gravity to maintain the self-stability in the water.

Because we confirmed sufficient water-tightness of the flange connections in the pilot study, the same flange connections were arranged on the shell structure of the demonstration machine. The two side turbine pods were connected by a cross beam structure. This cross beam structure was designed so that it has sufficient strength against the torque from the two generator turbines. In addition, finite element analysis was carried out to verify the strength against various loading conditions, including not only this torque from the turbines, but also the water pressure, the mooring force, the construction loads such as lifting load, and the wave loads in case of afloat and towing conditions.

The demonstration machine should have equivalent weight versus buoyancy to be efficiently operated beneath the sea surface. In addition, the positions of the center of gravity (and the center of buoyancy) is very important to maintain sufficient attitude stability of the floating body. Therefore, control and optimization of the weight distribution of the body and equipment is extremely important.

To achieve this, we employed a 3-dimensional CAD system for the design. Figure 6 shows the generated 3-dimensional model, comprising all the structures and equipment, such as structural members, welding bead, electrical controller, bolts and nuts, lubrication oil and so on. Fully utilizing this model, we could correctly assess the center of gravity of the entire floating body, and the layout design of the equipment considering stability was made possible.

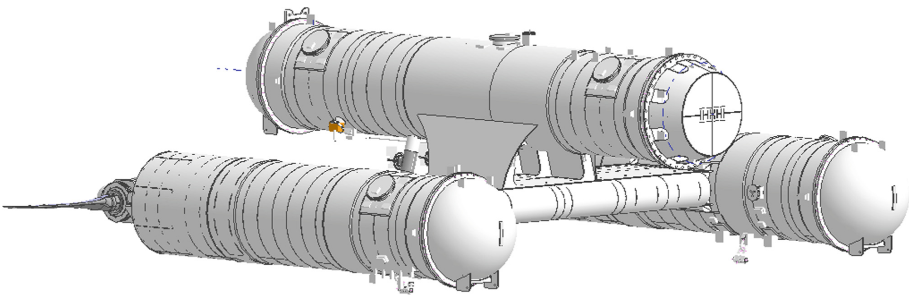

Fig. 6. 3-dimentional model of demonstration machine

3.2 Components

The demonstration machine has some heavy components, which cannot be easily installed inside the pods, because they are too heavy for manual handling and also the narrow tunnel-like pod tube structure prohibits usage of cranes. So we divided the overall body into some sub units which can be assembled outside the floating body, and realized work reduction for assembly in the tunnel. An example of sub unit division is indicated in Fig. 7.

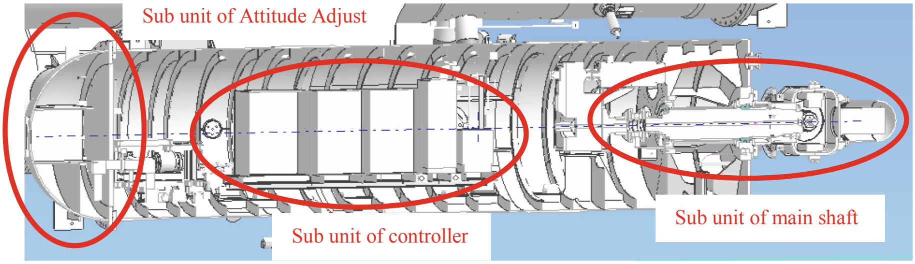

Fig. 7. Example of sub unit division (inside view of left side pod)

These main components and sub units are indicated below and in Fig. 8. Figure 9 shows the overview picture of the demonstration machine “KAIRYU” in the sea.

- Buoyancy adjustment device; ballast water management system controls the weight of demonstration machine.
- Attitude adjustment device; ballast shifting among three pods changes the position of center of gravity to prevent trim and heel.
- Generator; permanent magnet synchronous generators can make variable torque, which controls the turbine rotation speed at any current velocity.
- Blade pitch control device; pitch angles of 4 turbine blades can be controlled independently.
- Mooring line; HMPE rope has high strength, low elongation and light weight.
- Power cable; Electricity is transmitted through riser cable and subsea cable. They also include optical fiber cable. Therefore, monitoring of signals from each instrument and actuator is possible at the shore side.

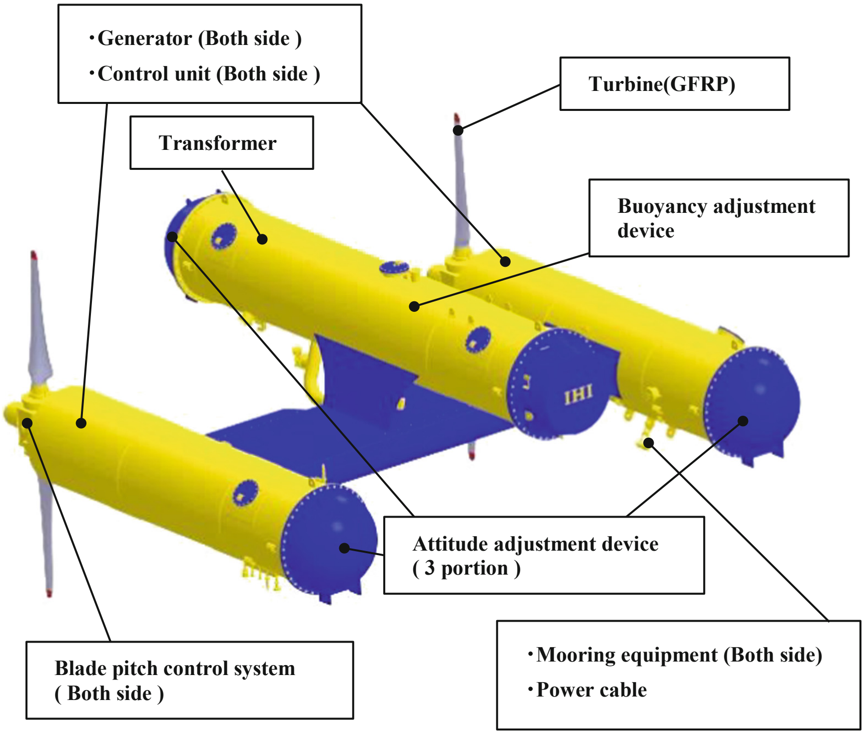

Fig. 8. Main components of demonstration machine

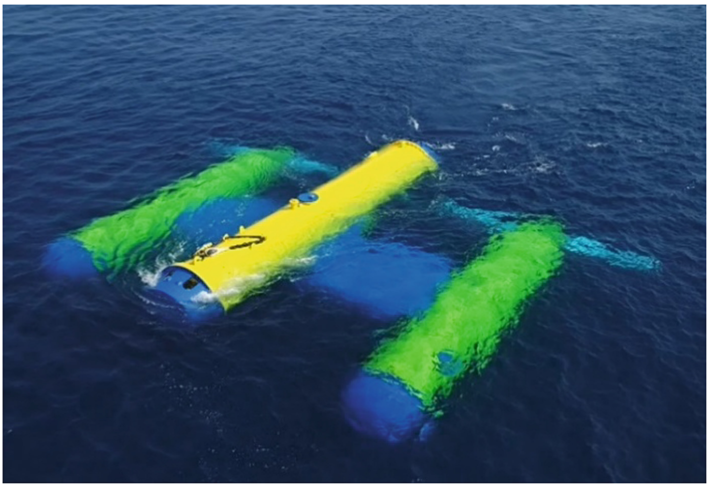

Fig. 9. Demonstration machine of ocean current turbine system, “KAIRYU”

3.3 Specifications and Capacity of Demonstration Machine

We designed and constructed the demonstration machine based on the considerations as mentioned above. This demonstration machine was named "KAIRYU" after voting by the children living near the field of the demonstration test. The specifications of this demonstration machine are indicated below, and Fig. 10 shows the overall picture of the demonstration machine.

Specifications and Capacity

- Power generation capacity: Max.100 kW (50 kW $\times$ 2)
- Rated current velocity: 1.5 m/s
- Assumed current velocity range for power generation: 0.5 – 2.0 m/s
- Turbine diameter: 11 m
- Length of main body: About 20 m
- Width of main body: About 20 m
- Total weight of body: About 380 tons
- Floating depth: 20–50 m/s
- Transmission voltage: 6600 V
- Distance of the moorage from shore: Max. 10 km
- Assumed Service life: 20 year
- Assumed maintenance cycle: 1 year

Fig. 10. Picture of the demonstration machine manufactured actually

4 Demonstration Test

4.1 Overview of the Demonstration Test

Towing tests and mooring tests were performed using the demonstration machine "KAIRYU". In the towing test conducted first, sensors and actuators are adjusted to make sure that the balance of the machine in the water keeps stable. In this test, we collected the data on the generated electric power from the turbines up to its maximum magnitude of 100 kW.

In the subsequent mooring test, we installed "KAIRYU" in the actual Kuroshio Current, and confirmed its practical power generation capability on site. As a result, we could obtain the rated output and the performance of the designed power generation (about 30 kW at the current speed of 1 m/s).

Moreover, various data were collected in the demonstration tests for further use and feedback to the future design of larger practical application. These include confirmation of the performance of the attitude control system, confirmation of the installation and removal method of the floating body, to name a few.

4.2 Towing Test (Performance Test)

Arrangement of the towing test is shown in Fig. 11. A gravity base anchor was hung from the barge at the depth of about 100 m. In order that relative arrangement will be same as that of the mooring test, KAIRYU was tethered to the anchor, and was towed by a tug together with the barge. This towing test was conducted in the west area of Kagoshima Prefecture (Fig. 12).

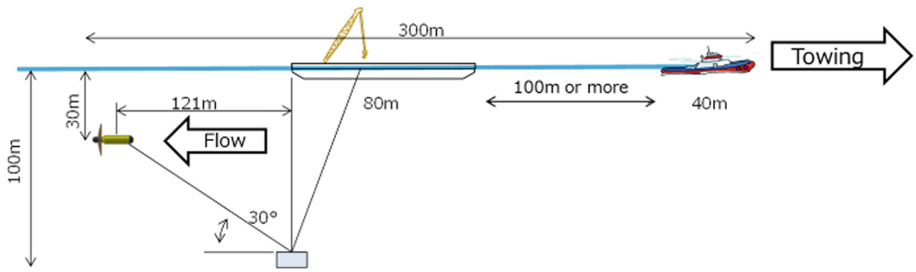

Fig. 11. Arrangement of towing test

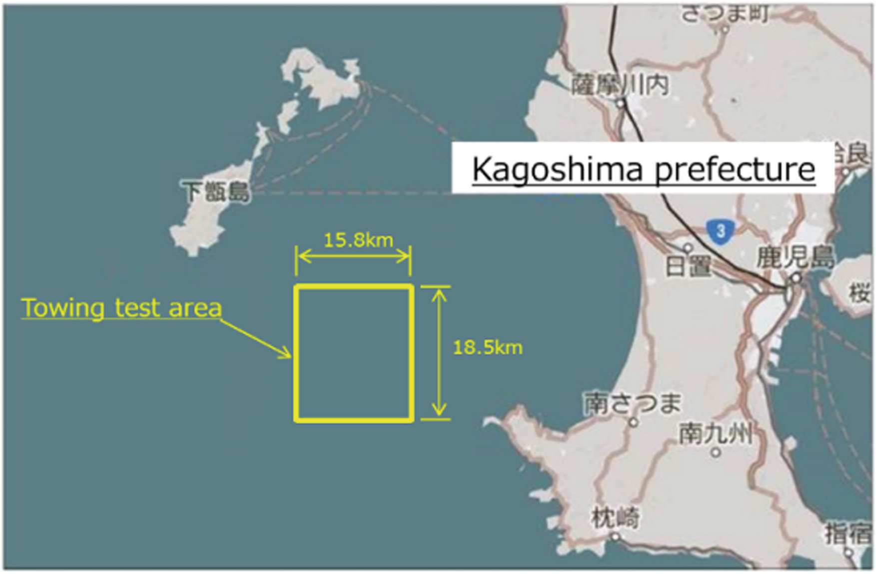

Fig. 12. Towing test area

4.3 Mooring Test

The site of the mooring test was the northern area of Kuchinoshima Island (Fig. 13). This area is designated as the "demonstration field of the ocean renewable energy" by the government, and is suitably organized by the local government for this kind of

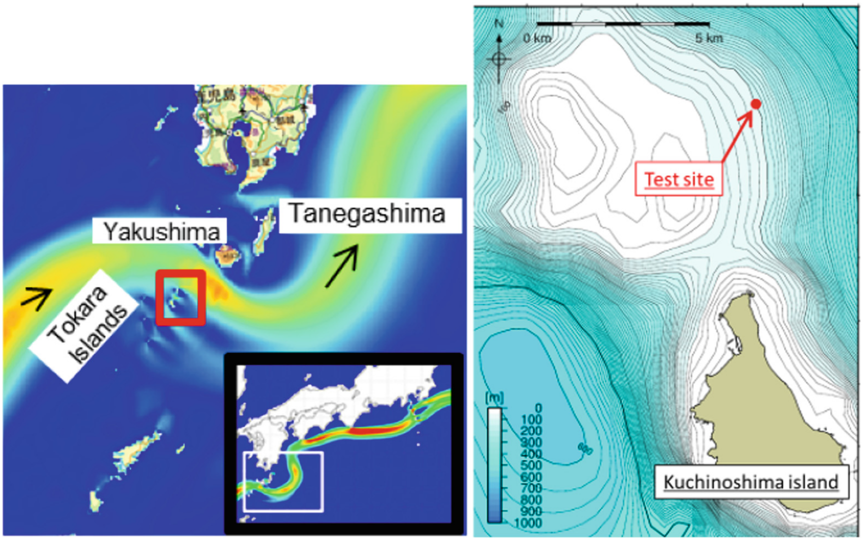

Fig. 13. Mooring test site

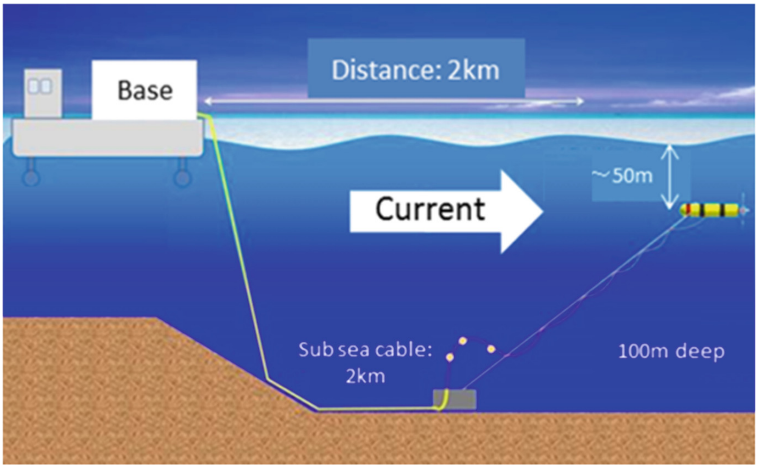

Fig. 14. Arrangement of mooring test

demonstration test. The arrangement of the demonstration test is shown in Fig. 14. KAIRYU was installed at the test point and moored by line anchored to the bottom of the sea. The electric power generated by turbine flows through the riser cable and the subsea cable, and is finally transmitted to the base on the barge.

4.4 Test Results

Power generation performance at various velocities was obtained in the towing test. The relation between the power generation and the current velocity in the towing test is shown in Fig. 15. The obtained results are observed to agree well with the designed power curve. In the mooring test, KAIRYU generated approximately 30 kW output at the current velocity of approximately 1.0 m/s in the actual Kuroshio Current. This also agrees well with the designed performance.

With regard to the floating stability performance in the Kuroshio Current, we confirmed the stability of depth and attitude in this demonstration tests. The time history of the measured depth and attitude is shown in Fig. 16, recorded in the mooring test when the operation phase changed from the waiting mode at the sea surface to the power generating mode. According to the results, we can confirm that KAIRYU has an excellent capability to follow the designated depth. In addition, the maximum angle of attitude inclination was kept within approximately 5°, which means high stability. Throughout the mooring test, we could control KAIRYU's depth within the target range and attitude inclination angle within ±10°. This high stability comes from the positional relation between the center of gravity and the center of buoyancy. Thus, active control by the attitude adjustment device was not used continuously, but only when it is needed.

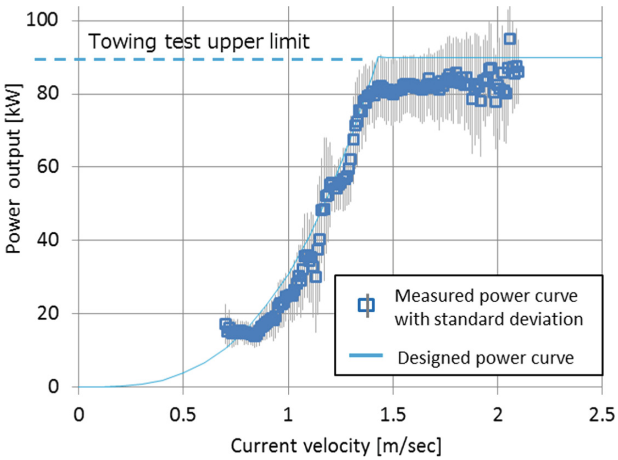

Fig. 15. Comparison of power curve between measured result and designed value

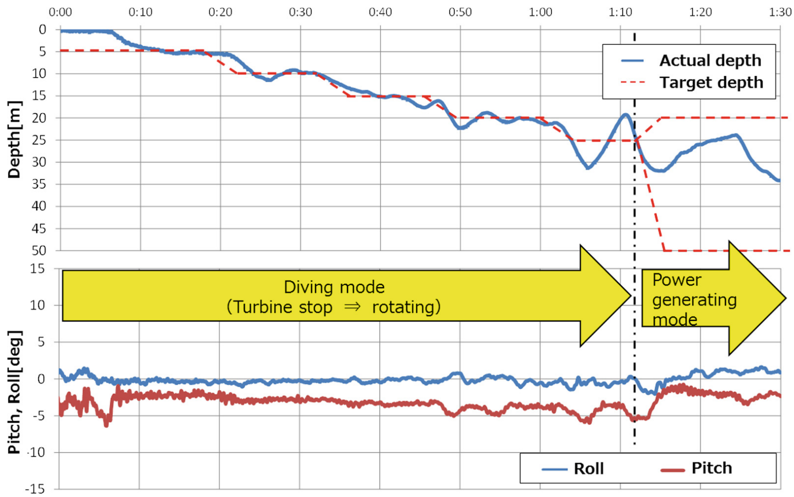

Fig. 16. Depth and attitude (roll/pitch)

Regarding the installation of the mooring test, KAIRYU was conveyed to an area near Kuchinoshima and installed with gravity base anchor, mooring line and power cable (see Fig. 17). The process of installation including laying down the subsea cable was completed in 3 days. This quick installation was achieved by the simple mooring configuration of this floating type power generation system.

Fig. 17. Installation beside Kuchinoshima Island

5 Study on the Structural Strength

Strength design of the floating body structure is very important to lead the demonstration test to a success without any troubles. To ensure this, we conducted a mock-up test and finite element analysis before the more large-scale demonstration test, as we have already touched upon in Sect. 2.4. In this chapter, we review the strength aspect of the turbine floater. First, the results of the mock-up test is discussed in comparison to the results of finite element analysis. Then, the strain measurement results of KAIRYU in the demonstration tests are shown and discussed again comparing with the results of finite element analysis.

5.1 Mock-Up Test of Structure for Water-Tightness

The pressure-resistant design of the shell structure to secure water-tightness in the deep sea is very important. Water-tightness of the flange connections is also essential, while several flange connections are inevitable for access man holes and other parts on the shell structure to enable human access and installation and/or removal of equipment. The mock-up model was fabricated to be tested for the strength and water-tightness as shown in Fig. 18. The diameter of the tube, structural arrangement and flange

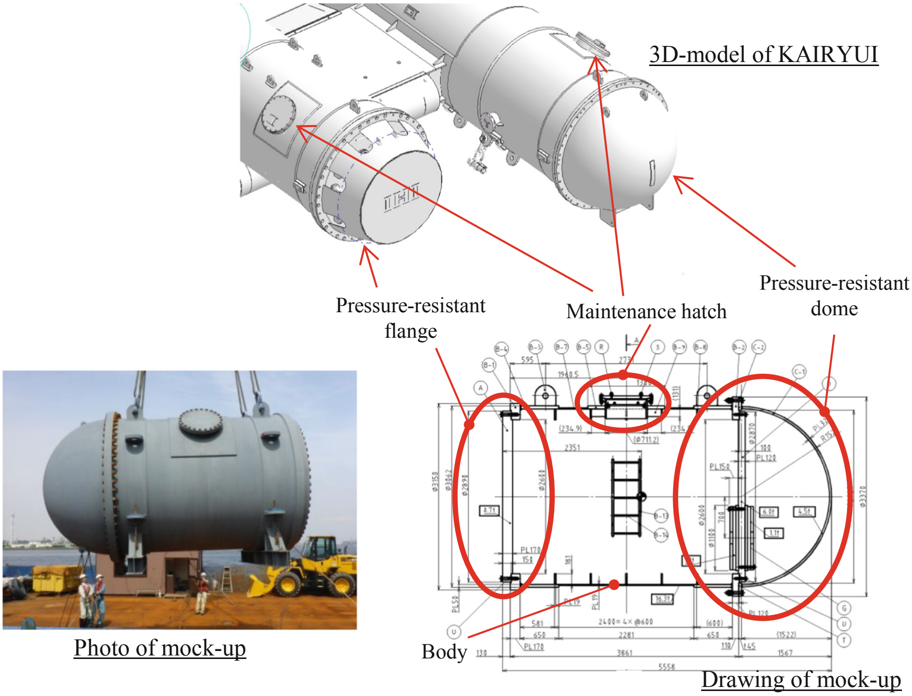

Fig. 18. Mock-up model of the shell structure

connections were determined to be as similar to the demonstration machine as possible. Then, this mock-up model was put into the pressure test at the water depth of 100 m.

5.2 Results of Mock-up Test

The mock-up model was instrumented with strain gauges inside the shell, and was submerged into the deep sea of about 100 m depth. Figure 19 shows the arrangement of the strain gauges. Strains were measure continuously throughout the process of changing the water depth of the mock-up, where the depth was changed as shown in Fig. 20. Submersion trials were carried out twice in this procedure as shown in the figure. The measured strain data were collected after the mock-up was uplifted onboard. Figure 21 plots the measured strain at each sensor location during the first submersion trial, taking the water depth in the abscissa.

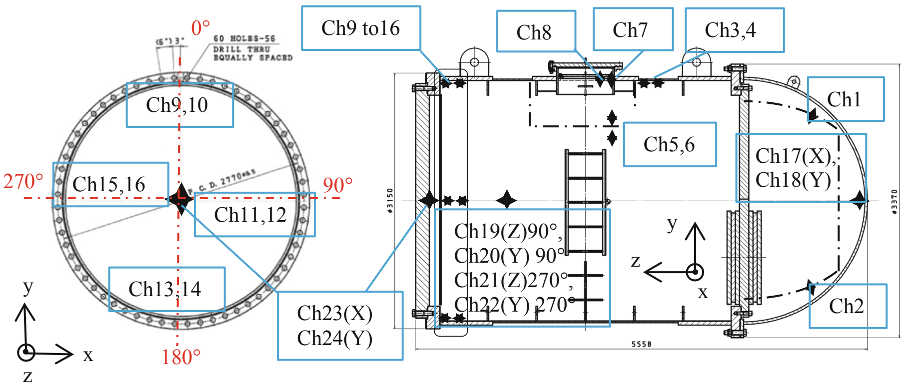

Fig. 19. The arrangement of stress sensors

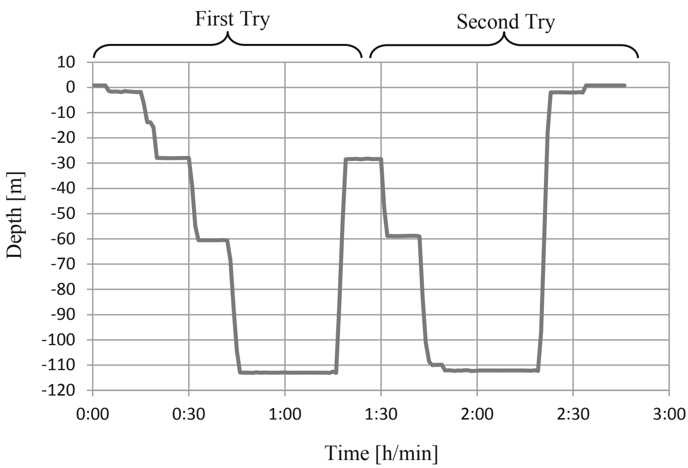

Fig. 20. Time chart of depth

We can observe in Fig. 21 that the measured strain changes in proportion to the water depth. Figure 22 shows the stress contour and the displacement of the structure obtained by finite element analysis conducted under the water pressure at the largest depth of 113 m during the test. Comparison between the results of FEM and the actual measurement is shown in Fig. 23 on the same condition of the water depth of 113 m. The afloat condition (the condition where the mock-up is afloat still on the water) was regarded as the initial condition and the value of the strain was calibrated to be zero in the initial condition.

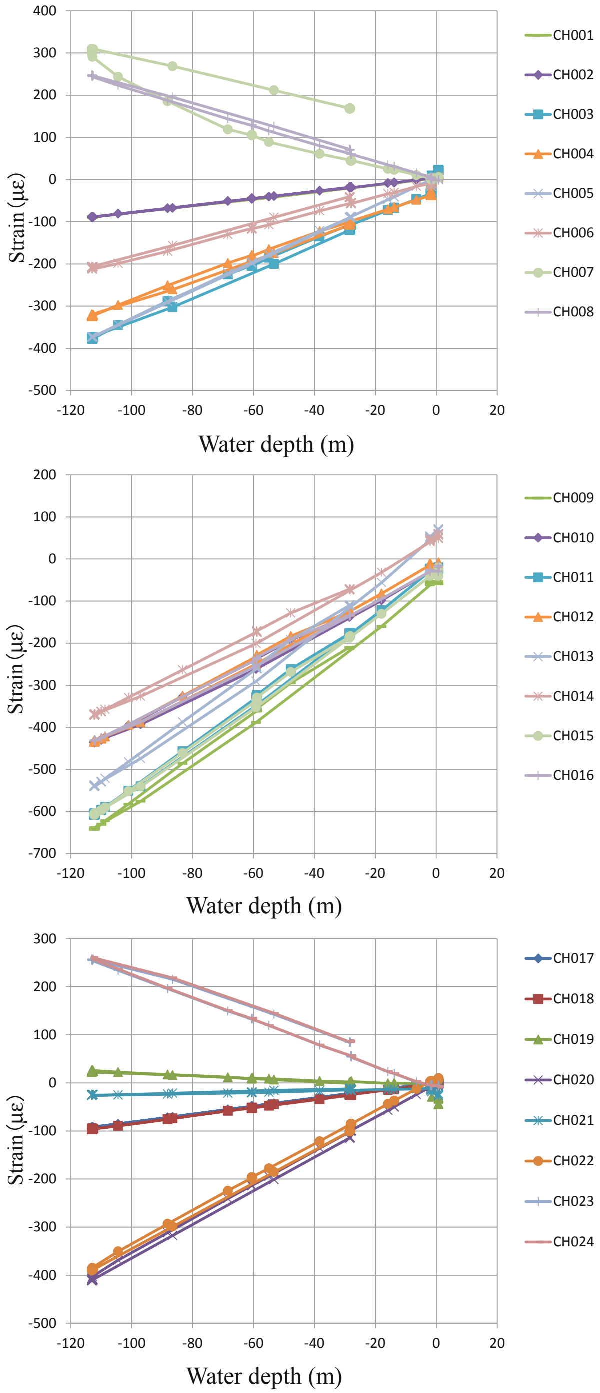

Fig. 21. Relation between measured strain and water depth

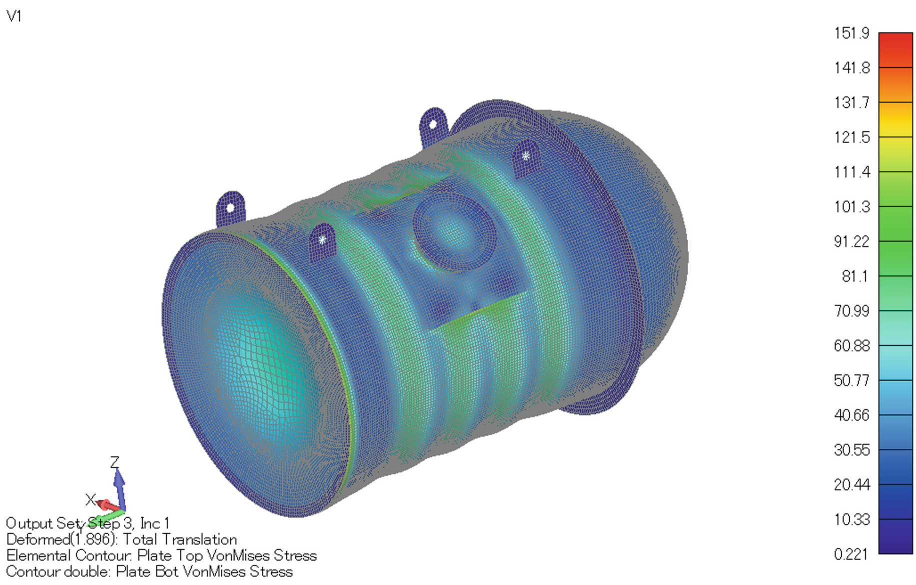

Fig. 22. Stress contour and displacement (FEM)

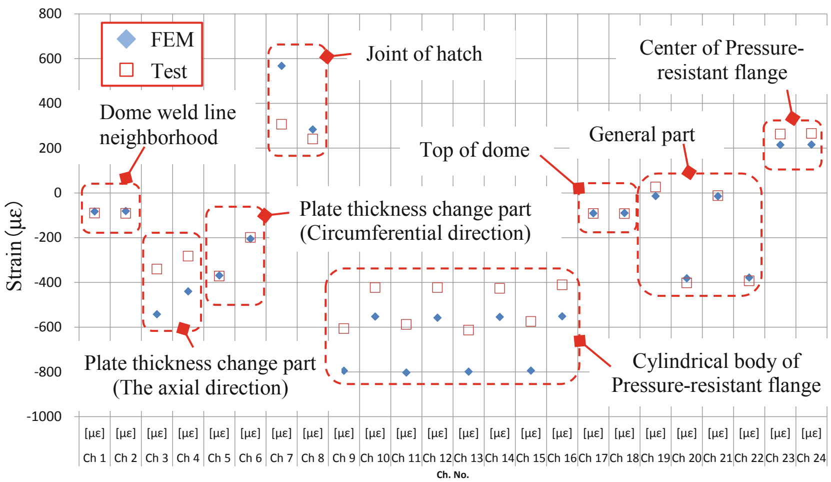

Fig. 23. Comparison of strain between FEM and the actual measurement

We can observe from Fig. 23 that the measured strain agrees well with that of FEM in way of the general part of the body and the hemispheric end part of the body. However, agreement was relatively worse in way of the locations close to the welding line of hatches and flanges or where the shell thickness changes. With regard to the locations close to the welding line, the strain gauges were instrumented at the location 1.5 times plate thickness apart from the weld toe, while stresses from FEM were picked out at the location 1.5 times plate thickness apart from the intersection of the crossing shell elements because the plate thickness and the weld bead are not modeled in FEM. This may have caused the discrepancies in the strain between measurement and FEM, especially when the plate thickness is large. In this sense, the results of FEM give conservative results.

5.3 Strength Design of the Floating Body

In the previous section, it was confirmed that we can conservatively assess strength of the floating structure using FEM. Then, we apply the identical method to the structural design of the demonstration machine. Design load cases are indicated in Table 1. To the conducted demonstration test, it is considered that the condition "Normal operation" applies. Therefore, comparison is made between the results of strain measurement and the results of FEM assuming normal operation condition under the current velocity of 1.5 m/s corresponding to the rated output and water depth of 50 m. An example of the analysis results in normal operation is shown in Fig. 24.

Table 1. Load cases

No.	Condition	Location of the float	Loading condition
1	Start-up	Surface of the sea	Zero water pressure and Full of ballast water
2	Normal operation (Electricity generation)	Undersea	Max. water pressure and Max. thrust load of blade
3	One side failure	Undersea	Max. water pressure with one side turbine blades lost
4	Stop	Undersea	Max. water pressure and Zero thrust load of blade
5	Stand-by	Surface of the sea	Zero water pressure and Zero thrust load of blade
6	Maintenance or installation	Land or on the barge	1) Lifting load 2) Lifting + wind load 3) Static load standing still on land 4) Heeled condition on the barge 5) Longitudinal inclination on the barge

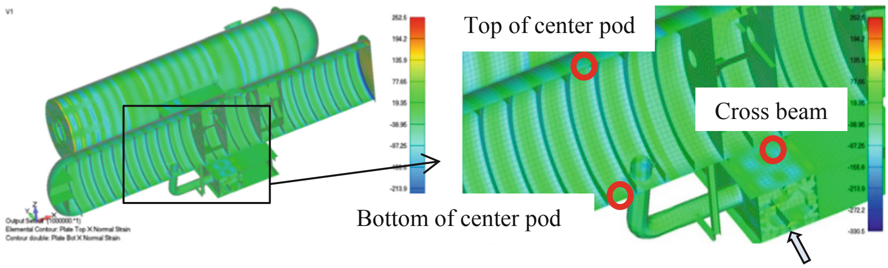

Fig. 24. Stress contour of FEM (The red circle shows the strain measurement points)

5.4 Locations of Strain Measurement

As shown by the red circles in Fig. 24 and Fig. 25, the strain measurement was conducted on the shell of the central pod and the cross beam inside the floating body. FBG (Fiber Bragg Grating) sensors were applied to avoid adverse effect of electro-magnetic noise in the measurement.

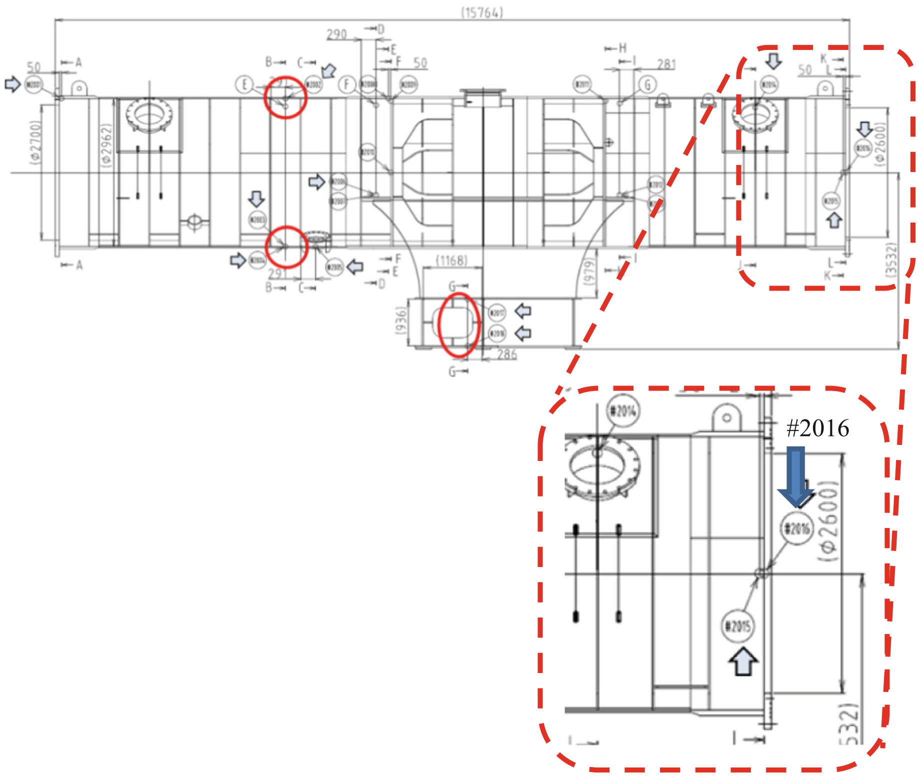

Fig. 25. Measurement location of the floating body (central pod and cross beam)

5.5 Results of Strain Measurement

As to the magnitude of the measured strain, zero point is not clear, and therefore, only the change in the magnitude should be evaluated. The primary factor exerting large strain in the floating body is the static water pressure in case of this demonstration test. Therefore, we calculated differences between the measured strains at two different water depths, and compared them with the results of FEM under the water pressure equivalent to this difference in water depth. Here we use the measured strains corresponding to two water depths 40 m and 10 m in the mooring test. Time history of the floating body water depth is indicated in Fig. 26. Measured strains in water depth of 40 m and water depth of 10 m are tabled in Table 2 in combination with the analysis results. The timings of the two different water depths were chosen as close as possible as indicated in Fig. 26 to exclude influences of the fluctuation of the conditions other than the water depth.

Figure 27 shows the relation between the floating body water depth and the measured strain. We can observe linear relationship between the water depth and the strain as a whole. Nonlinearity is observed when the water depth is small. This may be attributed to the action of waves and floater motions.

Furthermore, strain gauges were also installed at some other locations including structural discontinuity with large stress concentration. Among them, the maximum von Mises stress was about 52 MPa at the water depth of 45 m in way of the strain gauge #2016 located at the right end of Fig. 25, showing sufficient margin to the yield stress.

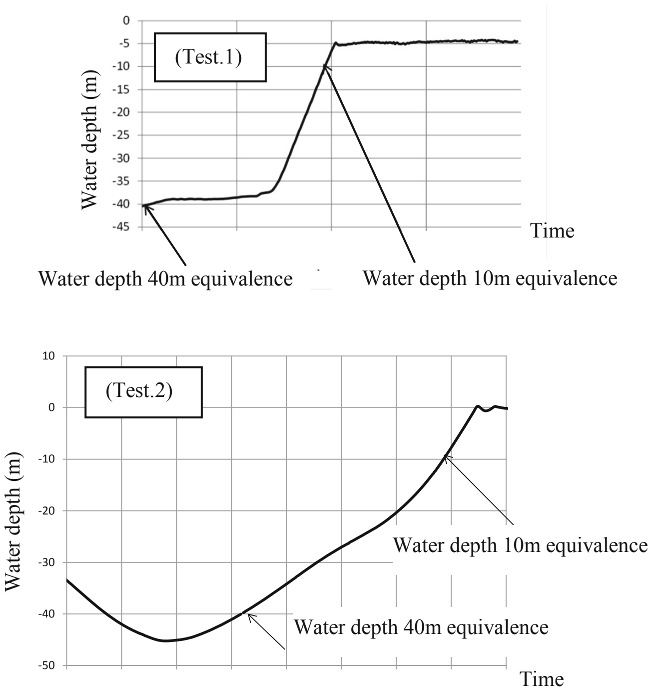

Fig. 26. The floating body depth chart as time change

Table 2. Measured and analyzed strains at each depth

(1) Water depth 40 m (unit: micro-strain)			
Portion	Test.1	Test.2	Analysis
Circumferential direction of bottom of center pod (#2003)	–200	–202	–132
Axial direction of bottom of center pod(#2004)	–72	–78	17.6
Axial direction of top of center pod(#2002)	–14	–16	–5.6
Top of beam structure(#2017)	28	18	81.3
Bottom of beam structure(#2018)	25	24	66.3
(2) Water depth 10 m (unit: micro-strain)			
Portion	Test.1	Test.2	Analysis
Circumferential direction of bottom of center pod (#2003)	–73	–80	–33
Axial direction of bottom of center pod(#2004)	–60	–60	4.4
Axial direction of top of center pod(#2002)	4	5	–1.4
Top of beam structure(#2017)	–21	–31	20.3
Bottom of beam structure(#2018)	–25	–23	16.6

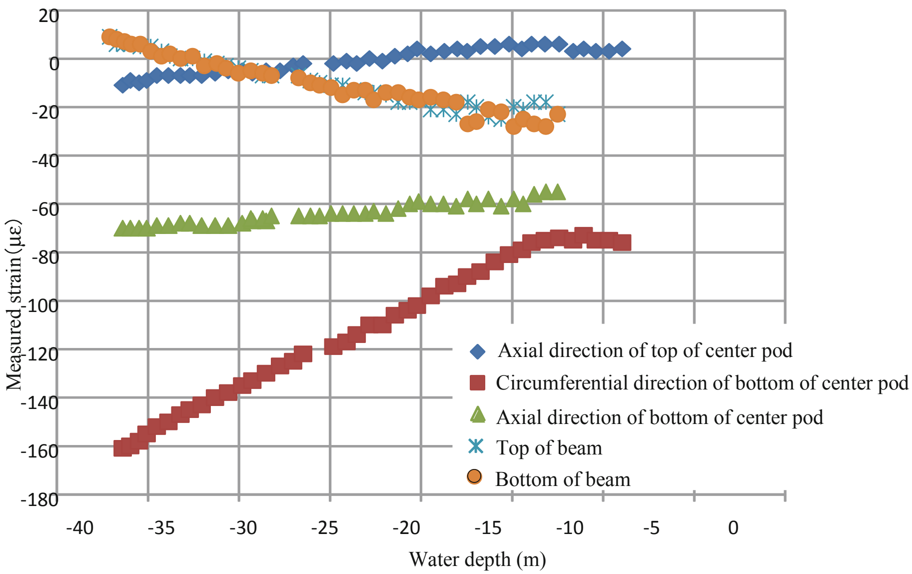

Fig. 27. Relation between the floating body water depth and the strain (test 1)

5.6 Comparison Between Strain Measurement and Analysis

Figure 28 shows the comparison between the measured strain and the results of FEM. The vertical axis shows the difference of the strains between the water depth of 40 m and the water depth of 10 m, corresponding to the water head of 30 m at the center of the generator pods. The FE analysis was also carried out under the static pressure of 30 m head at the center of the generator pods, in combination with the other loads such as thrust forces at 60% of the rated output.

From this figure, we can observe that the measured strains agree quite well with the results of the FEM. Regarding the axial stress of the center pod, although the absolute difference in the strains is not so significant between the measurement and the analysis, the ratio of the strains between them is far from 1.0. At this location, uniform axial compressive strain and local tensile strain on the inner surface of the shell plate due to the bending under outer pressure cancel each other, and the resulting strain is very small. This may have caused this relatively larger error at this location.

In this chapter, we carried out comparison between the strains measured in the mock-up test as well as the demonstration mooring test and the strains obtained by the FE analysis. As a result, good agreement between them was observed, and we could confirm the validity of the design method.

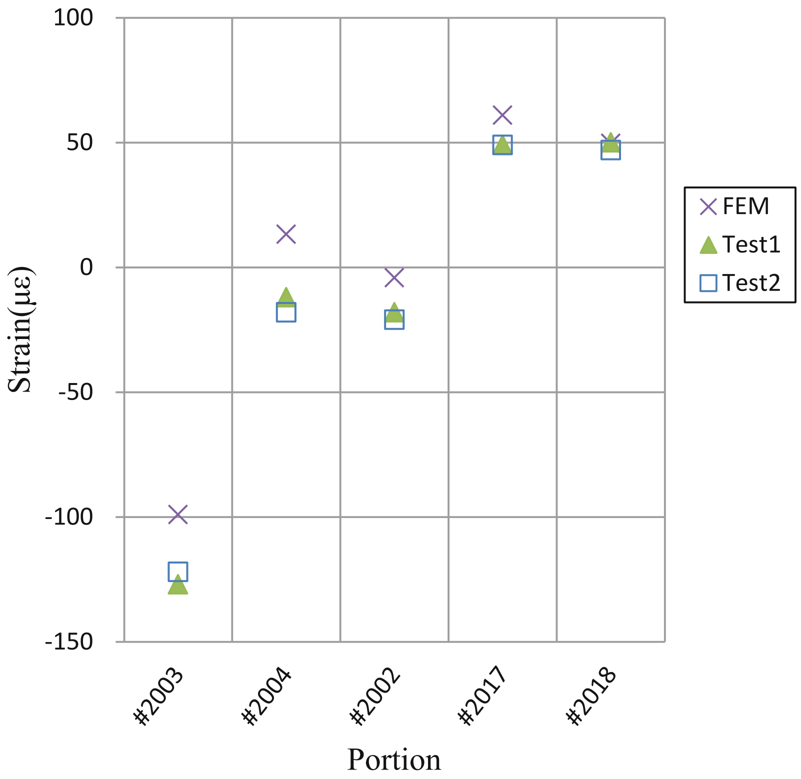

Fig. 28. Comparison of analysis results and measured values

6 Conclusion

We designed and constructed the floating type ocean current turbine system "KAIRYU", and conducted a world's first 100 kW class demonstration test in the actual Kuroshio Current site. As a result, the following concluding remarks are made.

- It was confirmed that KAIRYU can be controlled stably in the natural Kuroshio Current with regard to required depth and attitude.
- Actual power output of KAIRYU in the towing test and in the ocean current was in good agreement with the designed power generation.
- Strain on the structure was measured in the mock-up in the static pressure condition as well as KAIRYU in the operating condition, and was compared with the results of FEM. Good agreement was observed in general, and it was confirmed that the strength assessment method is adequate to be used for further development of a larger practical turbine floater.

References

1. Chen, F.: Kuroshio power plant development plan. Renew. Sust. Energ. Rev. **14**, 2655–2668 (2010)
2. Finkl, C.W., Charlier, R.: Electrical power generation from ocean currents in the Straits of Florida: Some environmental considerations. Renew. Sust. Energ. Rev. **13**, 2597–2604 (2009)
3. Shirasawa, K., Tokunaga, K., Iwashita, H., Shintake, T.: Experimental verification of a floating ocean-current turbine with a single rotor for use in Kuroshio currents. Renew. Energ. **91**, 189–195 (2016)
4. Lo, H.Y., Chen, J.H., Hsin, C.Y., Chiu, F.C.: Dynamics of floating Kuroshio turbine system in deployment, 29th Asian-Pacific Technical Exchange and Advisory Meeting on Marine Structures (TEAM 2015), pp. 169–176. Vladivostok, Russia (2015)
5. Lai, S.A., Hsin, C.Y., Lee, C.F., Lin, T.Y., Chen, J.H.: The floating Kuroshio turbine blades geometry design with consideration of the structural strength, 31st Asian-Pacific Technical Exchange and Advisory Meeting on Marine Structures (TEAM 2017), pp. 671–677. Osaka, Japan (2017)